Origin of faceted surface hillocks on semi-polar (11$\bar{2}$2) GaN templates grown on pre-structured sapphire

Yisong Han[1], Marian Caliebe[2], Menno Kappers[1], Ferdinand Scholz[2], Markus Pristovsek and Colin Humphreys[1]

[1]Department of Materials Science and Metallurgy, University of Cambridge, 27 Charles Babbage Road, Cambridge CB3 0FS, United Kingdom

[2]Institute of Optoelectronics, Ulm University, Albert-Einstein-Allee 45, 89081 Ulm, Germany

Corresponding author:

Dr Yisong Han, Email: yh241@cam.ac.uk, tel: +44(0)1223 767930 (office), +44(0)7908 162796 (mobile)

Abstract

The microstructure of semi-polar (11$\bar{2}$2) GaN templates grown on pre-structured r-plane sapphire by metal-organic vapor phase epitaxy (MOVPE) followed by hydride vapor phase epitaxy (HVPE) has been characterised by transmission electron microscopy (TEM). It is found that dislocations originating from the inclined c-plane-like GaN/sapphire interface bend and then terminate either at the coalescence regions of the adjacent GaN stripes or at the SiO_2 mask. However, the regions associated with the coalescence event during the MOVPE growth act as a source of dislocations and stacking faults in the subsequent growth process. More importantly, a direct link between the formation of a surface hillock, the presence of an inversion domain, and the preferential nucleation of randomly oriented GaN particles at a region containing a dislocation bundle originating from coalescence has been established. It is suggested that controlling the surface conditions of the MOVPE GaN layer before HVPE and optimising the HVPE nucleation process are important to avoid the surface hillocks.

Keywords

A1: Characterization. A1: Defects. A3: Hydride vapor phase epitaxy. A3: Metalorganic vapor phase epitaxy. B1: Nitrides. B2: Semiconducting III-V materials.

1. Introduction

There is a lack of efficient GaN based light emitting diodes (LEDs) emitting in the green to yellow region in comparison with the availability of efficient red and blue LEDs [1, 2]. This is known as the "green gap" problem and has been partially attributed to the presence of the built-in electric fields in InGaN quantum wells (QWs) grown in the c-direction [3]. Such internal electric fields arise from spontaneous and piezoelectrically generated charges in compressively stressed QWs, which cause a local separation of

electrons and holes and a longer radiative recombination time [4, 5]. The fields may be completely eliminated by growing the QW structures on non-polar planes (planes perpendicular to the c-plane) or reduced on semi-polar planes (inclined planes between the c-plane and a non-polar plane) [3, 4].

Non-polar or semi-polar device structures including the first green InGaN-based laser diodes on bulk GaN substrates have been demonstrated [6, 7]. Such high-quality bulk GaN substrates are produced by cutting from GaN boules and have, so far, a limited commercial potential due to their small size and high cost [8]. Non-polar or semi-polar GaN have also been grown heteroepitaxially on other substrate materials, such as non-polar a-plane ($11\bar{2}0$) and m-plane ($1\bar{1}00$) GaN on sapphire, $LiAlO_2$ and SiC, and semi-polar ($11\bar{2}2$) GaN on m-plane sapphire [9]. However, these heteroepitaxial films generally contain a high density of defects in comparison with conventional c-plane GaN grown on sapphire [10] and new and effective defect reduction approaches need to be developed [11]. Alternatively, a heteroepitaxial growth may still start from the c-plane, but on the inclined sidewalls of etched trenches [12]. In this case, a lower defect density is likely to be achieved, since the early stage of the growth essentially takes place along the c-direction, after which the individual stripes coalesce by a lateral growth and eventually form a semi-polar surface.

In this context, semi-polar ($11\bar{2}2$) GaN templates were grown on pre-structured r-plane ($10\bar{1}2$) sapphire substrates by two techniques: metal-organic vapor phase epitaxy (MOVPE) followed by hydride vapor phase epitaxy (HVPE). The MOVPE growth was stopped after the coalescence between the neighboring GaN stripes was complete. The HVPE process provides a much higher growth rate in comparison to MOVPE, enabling a quicker production of free-standing GaN substrates for the subsequent development of device structures [13]. The microstructure and the development of crystal defects in these samples were studied by transmission electron microcopy (TEM). In particular, the origin of surface hillocks was investigated by preparing thin foils exactly at the hillock centres using a focused ion beam (FIB).

2. Experimental

As detailed by Schwaiger [14], trenches were etched along the a-direction of r-plane sapphire, with the c-plane-like inclined sidewalls exposed to initiate the growth of GaN predominantly in the [0001] direction. The trenches are roughly 3 μm wide and 1.2 μm deep, and the period of the patterning is about 6 μm. The MOVPE GaN layer was deposited in a low-pressure horizontal flow Aixtron-200/4 RF-HT reactor using the standard precursors of trimethyl-gallium (TMGa), trimethyl-aluminium (TMAl) and high purity ammonia (NH_3). Generally, growth was started with an oxygen-doped AlN nucleation layer at a low temperature of about 960°C, followed by a GaN buffer layer at about 1105°C and then an *in-situ* SiN_x interlayer for defect reduction [15, 16].

Two samples with an MOVPE layer prepared under different conditions were investigated by TEM. For the first sample, the GaN growth continued at 1035ºC for 80 min, and then at 1005ºC for 30 min. The growth for the second sample continued at 1025ºC for 45 min and at 995ºC for 60 min. An earlier coalescence between the adjacent GaN stripes was achieved in the second sample as a result of the slightly lower growth temperatures used.

Before the samples were transferred into the HVPE chamber, the sample surface was cleaned using KOH and H_2SO_4:H_2O_2(1:1) solutions for 1 min and 4 min, respectively. The substrate temperature was slowly ramped up to 930ºC, at which the HVPE overgrowth was carried out. During the temperature ramping, a N_2 flow was maintained, with NH_3 gas injected at 700ºC and H_2 gas injected at 750ºC. Precursors GaCl and NH_3 were used at a V/III ratio of 18. A ~22 μm thick HVPE layer was deposited on the first MOVPE sample and a ~5μm HVPE layer was deposited on the second MOVPE sample. A schematic of the sample structure is shown in Figure 1, where the major crystallographic directions and planes for both GaN and sapphire are labeled.

Cross-sectional TEM specimens were prepared by conventional mechanical polishing, followed by Ar ion beam milling. The GaN wafers were cut perpendicular to the trenches, enabling observations along the m-direction of GaN. The Ar ion beam milling was performed in a Gatan PIPS (Precision Ion Polishing System) at an angle of 7° and a voltage of 5 kV. Cross-sectional TEM samples were also made by a focused ion beam (FIB) in a FEI Helios NanoLab SEM/FIB. The TEM samples were observed in a Philips CM30 microscope, operated at 300 kV.

3. Results and discussion

Figure 2a shows a cross-sectional overview of the first MOVPE/HVPE grown GaN template. It is composed of many two-beam bright-field images, recorded using $g = (11\bar{2}2)$ close to the $[1\bar{1}00]$ zone axis of GaN. Since the TEM sample is bent after Ar ion beam thinning, the tilting of the sample for each image was carefully adjusted to satisfy the above two-beam condition. According to the conventional invisibility criteria, a dislocation is invisible when $g.b = 0$ and g.bᴧu = 0 (where g is the operating reciprocal lattice vector and b is the Burgers vector of the dislocation) [17]. Therefore, all pure edge- and screw-type, and most mixed-type dislocations are in contrast. However, no basal-plane stacking faults (BSFs) are visible along this zone axis, since the $g.R$ products for all the associated reflections (R is the displacement vector of a BSF) are integers.

Figure 2a shows that the GaN layer is ~28 μm thick in total with a flat surface. The interface between the MOVPE GaN and the HVPE GaN exhibits some contrast, which is probably due to the presence of defects formed at the beginning of the HVPE growth. The coalescence regions between the neighboring GaN stripes are also visible as dark lines, running diagonally from top-left to bottom-right and extending to the top of the MOVPE layer. Figure 2b is a magnified view of the GaN layer in a sapphire trench, also recorded using the $(11\bar{2}2)$ reflection. It reveals that threading dislocations form at the inclined c-plane-like GaN/sapphire interface. Most of the dislocations bend 90° to either side at certain stages of the growth and terminate up at the coalescence regions or down in voids or on the SiO_2 mask. Thus, a low defect density is achieved before the start of the HVPE growth. The line direction of the dislocations after bending was confirmed to be along the [11-20] direction through tilting the TEM specimen by 17.4º to either the $[\bar{3}30\bar{1}]$ or the $[\bar{3}301]$ direction from the [1-100] zone [18].

However, at the HVPE/MOVPE growth interface, bundles of dislocations emerge from the GaN stripe coalescence boundaries and propagate to the top of the HVPE layer. In the example shown in Fig. 2a, the direction of the dislocation bundle formed in the HVPE layer is flipped into the a-direction by almost 90º from the line direction of the stripe coalescence boundary in the MOVPE-grown layer. BSFs also appear at the regions containing dislocation bundles, as revealed by images taken close to the $[11\bar{2}0]$ zone axis using the $(1\bar{1}00)$ reflection (Figure 3). It is found that most of dislocations within the dislocation bundles are directly associated with BSFs. g.b experiments confirmed that they are Frank-Shockley partial dislocations with a Burgers vector of the form of $\frac{1}{6}\langle 2\bar{2}03\rangle$, and the corresponding BSFs are I_1-type. The presence of a high density of dislocations and BSFs in the HVPE-grown GaN suggests that the coalescence boundaries between the stripes remain highly faulted and act as a source of defects in the HVPE layer.

Faceted hillocks were observed by SEM on the sample surface after HVPE GaN growth (Figure 4a), with the edge of the wafers exhibiting a significantly higher density. Most of them are larger than 50 μm across. In order to understand the mechanism of their formation, FIB was used to prepare $[1\bar{1}00]$ TEM thin foils exactly through the centres of some hillocks, as illustrated in Figure 4b. Figure 5a shows a bright-field image of a FIB sample, where two boundary structures propagating roughly along the c-direction were revealed (marked by black arrows, top right). Convergent beam electron diffraction patterns (CBED) were recorded from the regions inside (position 2 in Figure 5) and outside (positions 1,3 in Figure 5) the boundaries. There is an inversed asymmetry within the {0002} discs in the CBED patterns taken from position 2 relative to those from positions 1 and 3. This confirms that the crystal structure inside the two boundaries has an inversed crystallographic polarity and therefore it is an inversion domain.

In order to reveal the origin of the defects responsible for the formation of the hillocks, the sample with a thinner HVPE GaN layer of only ~5 μm was investigated. Hillocks also appear in this case, and the thinner HVPE layer enabled the focused ion beam to reach further inside the layers to where the hillocks nucleated. Figure 6 shows a bright-field image from a FIB sample also prepared along the $[1\bar{1}00]$ direction at the centre of a hillock. The presence of an inversion domain was again confirmed by CBED. In this case, the two domain boundaries form a right angle (labeled A and B). Boundary A is perpendicular to the c-direction, with boundary B being parallel to the c-direction. In addition, two particles were found located right beneath the inversion domain structure and above the MOVPE/HVPE interface (white arrow). Energy dispersive X-ray spectroscopy (EDX) analysis using a focused electron beam found Ga within the particles and no other elements (nitrogen is not detectable in our EDX system). CBED patterns were acquired from the particles in order to identify their lattice structure. Figure 6b and c show two CBED patterns taken from one of the particles along two different zone axes. The indexing of them with reference to the surrounding material confirmed the particles are randomly oriented GaN rather than other Ga related compounds.

The exact position of the GaN particles relative to the coalescence event in the MOVPE GaN layer was investigated using TEM samples prepared by mechanical polishing and Ar ion milling, which are thinner and exhibit a better contrast for defects within the layers than the FIB samples. Due to a slight change of growth conditions in this sample, the trace of coalescence in the MOVPE layer (marked by a white dashed

lines in Figure 6a) appeared different from the sample with a thicker HVPE layer. In this case, dislocation bundles (yellow dashed line in Figure 6a) started to appear from the inside of the MOVPE layer rather than from the HVPE/MOVPE interface. It is revealed that the GaN particles are located at the regions closely associated with a dislocation bundle originating from a coalescence region.

Based on the above observations, we suggest the following mechanism for surface hillock formation in the HVPE layer: at the start of the HVPE process, non-epitaxial GaN particles preferentially nucleate on the MOVPE GaN surface regions containing a high density of defects formed due to the coalescence process; these GaN particles then act as nucleation centres for inversion domains by interrupting the prevailing Ga-polar growth: the hillocks develop because of a higher growth rate of the inversion domain compared to that of the surrounding material.

Hillock structures are one of the common defects in GaN grown on the basal plane. When GaN is grown with a N-polar surface by homoepitaxy on a mechano-chemically prepared N-polar GaN template, pyramidal hillocks can appear [19-23]. Such pyramidal features have a Ga-polar inversion domain at their core, which grows faster than the N-polar matrix. It is found by TEM that the Ga-polar inversion domains nucleate at a thin layer of oxygen-containing material, possibly a contamination from the KOH cleaning procedure used prior to the growth [21]. Pyramidal hillocks have also been observed on GaN with a Ga-polar surface grown either by heteroepitaxy on sapphire or by homoepitaxy on GaN bulk templates [24-26]. These hillocks are understood to arise from a spiral growth around one or more dislocations with a screw component. Overall, it has been shown that the density of hillocks on c-plane GaN surfaces can be reduced by using GaN templates with a small miscut angle [19, 20, 25, 26]. In addition to polar GaN, hillock structures are reported on both semi-polar and non-polar surfaces. Hillocks on semi-polar GaN are again attributed to the formation of inversion domains [27], whilst those on non-polar m-plane GaN are associated with the presence of screw-component dislocations at their cores and can be removed by using m-plane GaN templates with a miscut angle along either the *a*- or *c*-directions [28, 29].

Similar to the results presented here, hillocks on semi-polar surfaces grown by HVPE/MOVPE on pre-structured sapphire have also been reported [30]. In this work, the formation of inversion domains is considered to be a direct consequence of the presence of randomly oriented GaN particles at the start of HVPE GaN growth, which preferentially nucleate near the stripe coalescence regions of the MOVPE-grown semi-polar $(11\bar{2}2)$ template. According to our observations, the density / distribution of hillocks varies from sample to sample and also varies across individual wafers. In addition, the cause of the inversion domains formed on semi-polar $(11\bar{2}2)$ GaN grown on $(10\bar{1}0)$ sapphire is considered to be closely related to the precursors used in the HVPE process and possibly reactor memory effects [27]. All the evidence indicates that the surface condition of the substrate and the surface diffusion and/or nucleation process at the beginning of the HVPE growth needs to be carefully controlled and optimised in order to produce high quality GaN templates free of hillocks.

4. Conclusions

TEM has been used to study the defects in semi-polar ($11\bar{2}2$) GaN templates grown on pre-structured sapphire. The propagation of dislocations has been observed from cross-sectional thin foils prepared by conventional mechanical polishing and Ar ion beam milling. There is a natural defect reduction mechanism in such templates during the MOVPE growth, where dislocations terminate as a result of the existence of a coalescence event. However, the coalescence regions act as a new source of defects, leading to the appearance of dislocation bundles. The origin of the formation of surface hillocks was studied from TEM samples made by FIB. We propose that at the start of the HVPE growth process, randomly oriented GaN particles form on the MOVPE GaN surface, which evolve into an associated inversion domain and finally a surface hillock. It is suggested that the hillocks may be avoided by improving the MOVPE GaN surface and/or growth conditions at the beginning of the HVPE process. The development of dislocations and the proposed formation mechanism of hillocks are illustrated in Figures 7a and b, respectively.

Acknowledgements

References

[1] S. Pimputkar, J.S. Speck, S.P. DenBaars, S. Nakamura, Prospects for LED lighting, Nature Photonics, 3 (2009) 179-181.

[2] C.J. Humphreys, Solid-state lighting, MRS Bull., 33 (2008) 459-470.

[3] J.S. Speck, S.F. Chichibu, Nonpolar and semipolar group III nitride-based materials, MRS Bull., 34 (2009) 304-312.

[4] J.-H. Ryou, P.D. Yoder, J. Liu, Z. Lochner, H. Kim, S. Choi, H.J. Kim, R.D. Dupuis, Control of quantum-confined stark effect in InGaN-Based quantum wells, IEEE J. Sel. Top. Quant. Electron., 15 (2009) 1080-1091.

[5] D.A.B. Miller, D.S. Chemla, T.C. Damen, A.C. Gossard, W. Wiegmann, T.H. Wood, C.A. Burrus, Band-edge electroabsorption in quantum well structures - the quantum-confined stark-effect, Phys. Rev. Lett., 53 (1984) 2173-2176.

[6] Y. Yoshizumi, M. Adachi, Y. Enya, T. Kyono, S. Tokuyama, T. Sumitomo, K. Akita, T. Ikegami, M. Ueno, K. Katayama, T. Nakamura, Continuous-wave operation of 520 nm green InGaN-based laser diodes on semi-polar {2021} GaN Substrates, Appl. Phys. Express, 2 (2009) 092101.

[7] D.F. Feezell, M.C. Schmidt, S.P. DenBaars, S. Nakamura, Development of nonpolar and semipolar InGaN/GaN isible light-emitting diodes, MRS Bull., 34 (2009) 318-323.

[8] S.F. Chichibu, M. Kagaya, P. Corfdir, J.-D. Ganière, B. Deveaud-Plédran, N. Grandjean, S. Kubo, K. Fujito, Advantages and remaining issues of state-of-the-art m-plane freestanding GaN substrates grown by

halide vapor phase epitaxy for m -plane InGaN epitaxial growth, Semicond. Sci. Technol., 27 (2012) 024008.

[9] F. Scholz, Semipolar GaN grown on foreign substrates: a review, Semicond. Sci. Technol., 27 (2012) 024002.

[10] C.F. Johnston, M.J. Kappers, C.J. Humphreys, Microstructural evolution of nonpolar (11-20) GaN grown on (1-102) sapphire using a 3D-2D method, J. Appl. Phys., 105 (2009) 073102.

[11] P. Vennéguès, Defect reduction methods for III-nitride heteroepitaxial films grown along nonpolar and semipolar orientations, Semicond. Sci. Technol., 27 (2012) 024004.

[12] N. Okada, K. Tadatomo, Characterization and growth mechanism of nonpolar and semipolar GaN layers grown on patterned sapphire substrates, Semicond. Sci. Technol., 27 (2012) 024003.

[13] K. Fujito, S. Kubo, I. Fujimura, Development of bulk GaN crystals and nonpolar/semipolar substrates by HVPE, MRS Bull., 34 (2009) 313-317.

[14] S. Schwaiger, PhD theses, Ulm University (2011).

[15] M. Caliebe, T. Meisch, B. Neuschl, S. Bauer, J. Helbing, D. Beck, K. Thonke, M. Klein, D. Heinz, F. Scholz, Improvements of MOVPE grown (11-22) oriented GaN on pre-structured sapphire substrates using a SiNx interlayer and HVPE overgrowth, Phys. Stat. Sol. C, 11 (2014) 525-529.

[16] J. Hertkorn, F. Lipski, P. Brückner, T. Wunderer, S.B. Thapa, F. Scholz, A. Chuvilin, U. Kaiser, M. Beer, J. Zweck, Process optimization for the effective reduction of threading dislocations in MOVPE grown GaN using in situ deposited masks, J. Cryst. Growth., 310 (2008) 4867-4870.

[17] J.W. Edington, Practical electron microscopy in materials Science, Van Nostrand Reinhold Co., 1976.

[18] P. Vennegues, B. Beaumont, V. Bousquet, M. Vaille, P. Gibart, Reduction mechanisms for defect densities in GaN using one- or two-step epitaxial lateral overgrowth methods, J. Appl. Phys., 87 (2000) 4175-4181.

[19] A.R.A. Zauner, E. Aret, W.J.P. Van Enckevort, J.L. Weyher, S. Porowski, J.J. Schermer, Homo-epitaxial growth on the N-face of GaN single crystals: the influence of the misorientation on the surface morphology, J. Cryst. Growth., 240 (2002) 14-21.

[20] A.R.A. Zauner, J.L. Weyher, M. Plomp, V. Kirilyuk, I. Grzegory, W.J.P. Van Enckevort, J.J. Schermer, P.R. Hageman, P.K. Larsen, Homo-epitaxial GaN growth on exact and misoriented single crystals: suppression of hillock formation, J. Cryst. Growth., 210 (2000) 435-443.

[21] J.L. Weyher, P.D. Brown, A.R.A. Zauner, S. Müller, C.B. Boothroyd, D.T. Foord, P.R. Hageman, C.J. Humphreys, P.K. Larsen, I. Grzegory, Morphological and structural characteristics of homoepitaxial GaN grown by metalorganic chemical vapour deposition (MOCVD), J. Cryst. Growth., 204 (1999) 419-428.

[22] G. Nowak, K. Pakuła, I. Grzegory, J.L. Weyher, S. Porowski, Dislocation structure of growth hillocks in homoepitaxial GaN, Phys. Stat. Sol. B, 216 (1999) 649-654.

[23] P.R. Hageman, V. Kirilyuk, W.H.M. Corbeek, J.L. Weyher, B. Lucznik, M. Bockowski, S. Porowski, S. Müller, Thick GaN layers grown by hydride vapor-phase epitaxy: hetero-versus homo-epitaxy, J. Cryst. Growth., 255 (2003) 241-249.

[24] W. Qian, G.S. Rohrer, M. Skowronski, K. Doverspike, L.B. Rowland, D.K. Gaskill, Open‑core screw dislocations in GaN epilayers observed by scanning force microscopy and high‑resolution transmission electron microscopy, Appl. Phys. Lett., 67 (1995) 2284-2286.

[25] F. Oehler, T. Zhu, S. Rhode, M.J. Kappers, C.J. Humphreys, R.A. Oliver, Surface morphology of homoepitaxia c-plane GaN: hillocks and ridges, J. Cryst. Growth., 383 (2013) 12-18.

[26] K. Zhou, J. Liu, S. Zhang, Z. Li, M. Feng, D. Li, L. Zhang, F. Wang, J. Zhu, H. Yang, Hillock formation and suppression on c-plane homoepitaxial GaN Layers grown by metalorganic vapor phase epitaxy, J. Cryst. Growth., 371 (2013) 7-10.

[27] T.J. Baker, PhD theses, University of California, Santa Barbara (2006).

[28] R.M. Farrell, D.A. Haeger, X. Chen, C.S. Gallinat, R.W. Davis, M. Cornish, K. Fujito, S. Keller, S.P. DenBaars, S. Nakamura, Origin of pyramidal hillocks on GaN thin films grown on free-standing m-plane GaN substrates, Appl. Phys. Lett., 96 (2010) 231907.

[29] A. Hirai, Z. Jia, M.C. Schmidt, R.M. Farrell, S.P. DenBaars, S. Nakamura, J.S. Speck, K. Fujito, Formation and reduction of pyramidal hillocks on m-plane {1-100} GaN, Appl. Phys. Lett., 91 (2007) 191906.

[30] K. Yamane, M. Ueno, K. Uchida, H. Furuya, N. Okada, K. Tadatomo, Reduction in Dislocation Density of Semipolar GaN Layers on Patterned Sapphire Substrates by Hydride Vapor Phase Epitaxy, Appl. Phys. Express, 5 (2012) 095503.
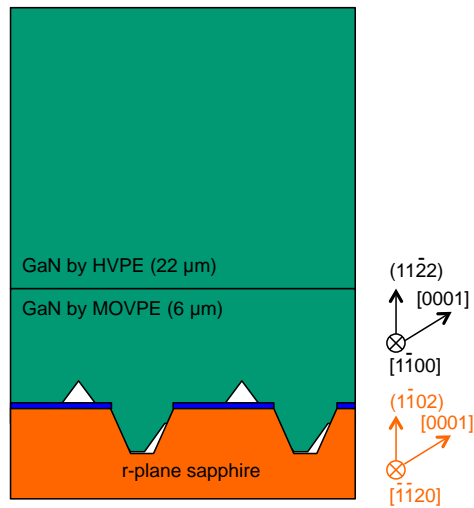
Figure 1. Structure of the GaN layers grown by MOVPE followed by HVPE (not to scale). The blue regions represent SiO_2 masks.
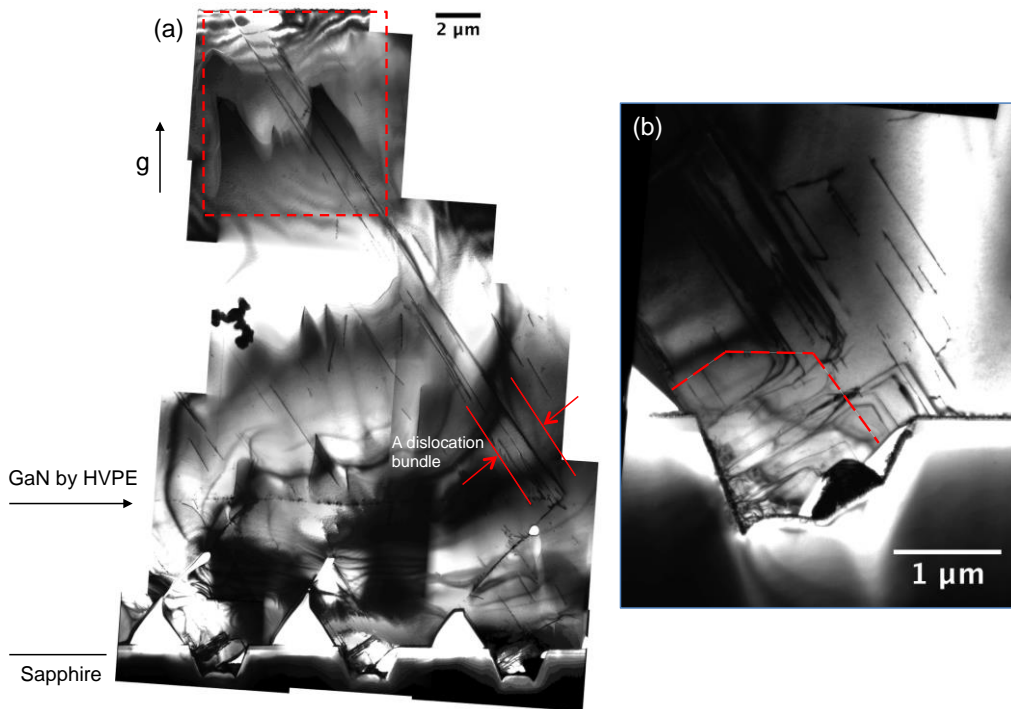

Figure 2. (a) Cross-sectional overview of a MOVPE/HVPE GaN template, showing the development of defects across the GaN layer. This micrograph is composed of many two-beam bright-field images recorded using $g = (11\bar{2}2)$ close to the $[1\bar{1}00]$ zone axis. The interface between the MOVPE GaN and HVPE GaN exhibit some contrast. (b) A magnified view of the GaN layer in a sapphire trench taken under the same diffraction contrast condition, showing dislocations originate from the inclined c-plane-like GaN/sapphire interface and bend towards either side as the growth progresses. The approximate position of the SiN_x interlayer is marked by a red dashed line.
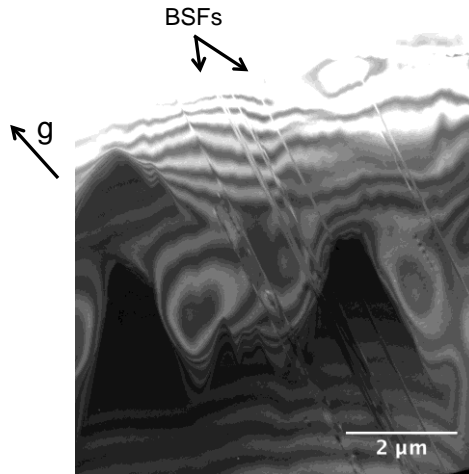
Figure 3. $(1\bar{1}00)$ two-beam bright-field image, taken close to the $[11\bar{2}0]$ zone axis from the marked region in Figure 2a.
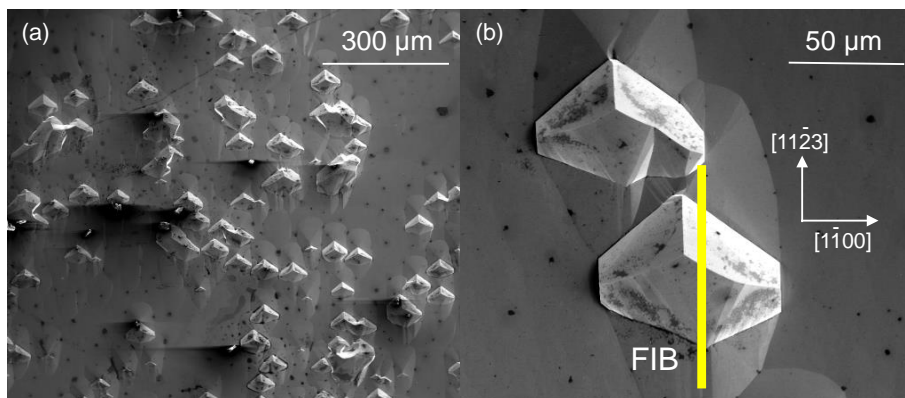

Figure 4. (a) Faceted hillocks observed on the sample surface by SEM. (b) $[1\bar{1}00]$ zone TEM thin foils were prepared using FIB at the centre of the surface hillocks, as marked by the yellow line.
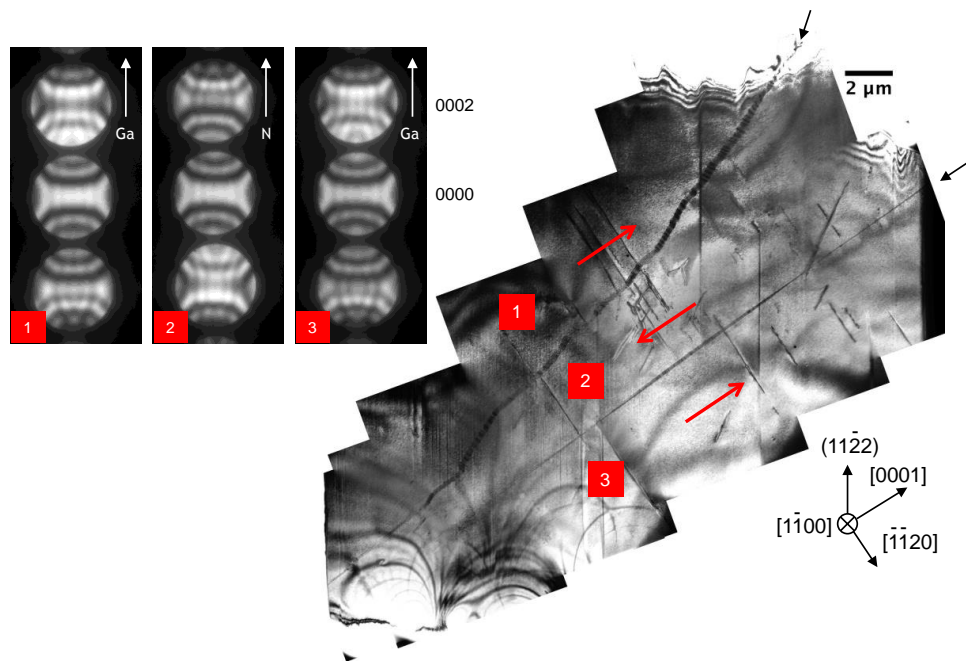
Figure 5. (11$\bar{2}$2) two-beam bright field image of a FIB sample prepared at the centre of a surface hillock, where two boundary structures were revealed. CBED patterns taken at positions 1, 2 and 3 are shown next to the TEM image. The CBED patterns were rotated for a better visualization.
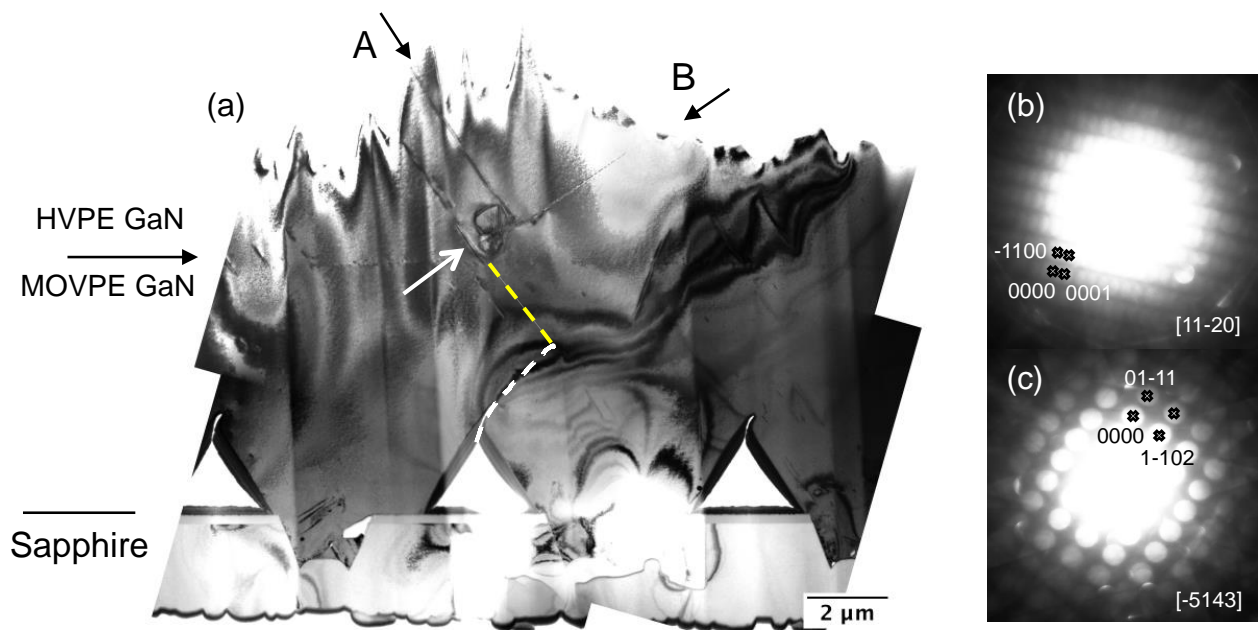

Figure 6. (a) Bright-field TEM image taken from a thin foil prepared using FIB at the centre of a surface hillock. This sample has a thinner HVPE GaN layer. The presence of an inversion domain structure and GaN particles was confirmed by electron diffraction. The trace of the coalescence event is marked by a white dashed line. (b,c) The indexing of the CBED patterns taken from the particles (arrowed) confirm that they are randomly oriented GaN.
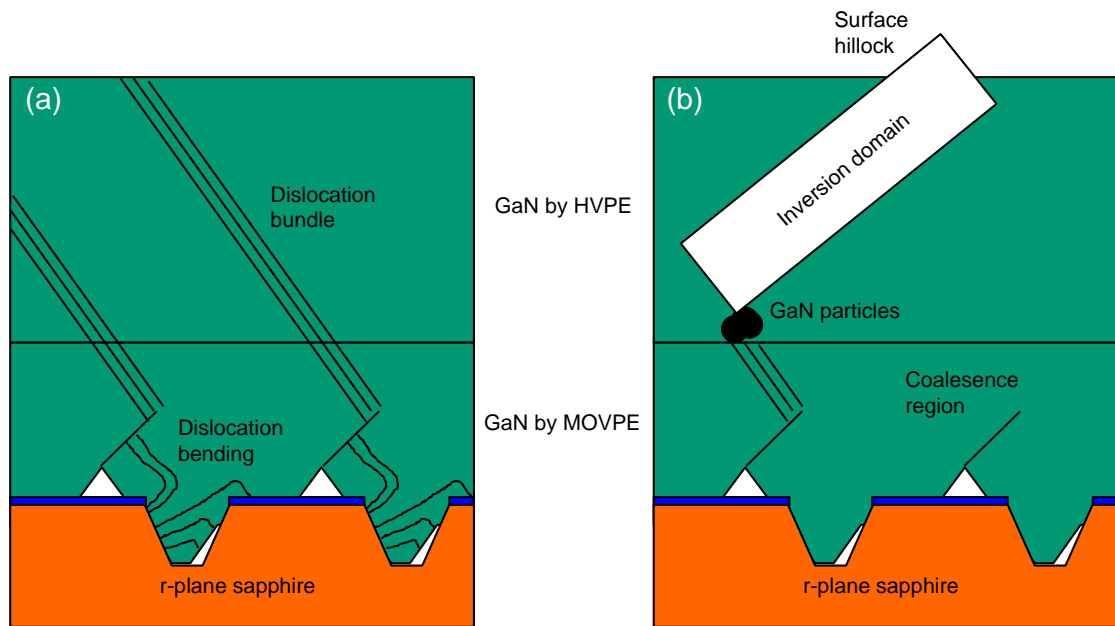
Figure 7. Schematics of (a) the development of dislocations and (b) the formation of hillocks (not to scale).